NJC

PAPER

View Article Online
View Journal | View Issue

Cite this: *New J. Chem.*, 2014, **38**, 1168

Hydrothermal synthesis and magnetic properties of $REFe_{0.5}Cr_{0.5}O_3$ (RE = La, Tb, Ho, Er, Yb, Lu and Y) perovskite

Long Yuan,[a] Keke Huang,[a] Changmin Hou,[a] Wenchun Feng,[b] Shan Wang,[a] Cuiping Zhou[a] and Shouhua Feng*[a]

Received (in Montpellier, France) 3rd September 2013,
Accepted 25th November 2013

DOI: 10.1039/c3nj01046e

www.rsc.org/njc

A low temperature, one-pot route to iron-doped rare-earth chromite perovskite was proposed. Fe half-doped rare-earth chromites, $REFe_{0.5}Cr_{0.5}O_3$ (RE = La, Tb, Ho, Er, Yb, Lu and Y) were prepared *via* a mild hydrothermal method and their magnetic properties were studied. All of these materials are well-crystallized and the profile refinement of powder X-ray diffraction (XRD) data showed that each of them adopts an orthorhombic distorted (*Pbnm*) perovskite structure. The temperature dependence of the magnetization curves indicate an improved order of arrangement of Fe^{3+} and Cr^{3+} at the B-site in some samples. Hysteresis measurements of $YFe_{0.5}Cr_{0.5}O_3$ indicate that saturated and remnant magnetization were improved greatly compared to that prepared *via* the solid state method.

Introduction

Electrical and magnetic properties of Fe-doped rare-earth (RE) chromites $REFe_{1-x}Cr_xO_3$ have been widely studied.[1–4] It was found recently that rare-earth chromites of the formula $RECrO_3$ (RE = Y, Ho, Er, Yb, Lu) exhibit canted antiferromagnetic (C-AFM) behavior at 113–140 K (T_N) and a dielectric transition at 472–516 K (T_E) providing a new family of multiferroics.[5] Fe half-doped rare-earth chromites may exhibit superior magnetic and electric behavior, which can also be confirmed by the magnetization of layered $LaCrO_3$–$LaFeO_3$ *via* the molecular beam epitaxy (MBE) method.[1] Ferroelectricity and the magnetoelectric effect at the magnetic ordering temperature (T_N = 260 K) of the transition metal ions (Fe^{3+} and Cr^{3+}) in $YCr_{0.5}Fe_{0.5}O_3$ were reported recently.[6,7] While both the end members, $YCrO_3$[8] (T_N = 140 K) and $YFeO_3$[9,10] (T_N = 640 K) exhibit weak ferromagnetism from a canted antiferromagnetic structure, they do not exhibit a dielectric anomaly or ferroelectric polarization at the magnetic transitions. According to the Kanamori–Goodenough (KG) rule, if Fe and Cr were in an ordered arrangement at the B-site, $Fe^{3+}(d^5)$–O–$Cr^{3+}(d^3)$ would show ferromagnetic (FM) behavior due to the superexchange interaction.[11,12] While, only antiferromagnetic was found in the reported systems of $REFe_{0.5}Cr_{0.5}O_3$ (RE = La, Y and Nd), as Cr and Fe ions were randomly distributed at the B-sites in the bulk samples.[13–15] To date, studies on the $REFe_{1-x}Cr_xO_3$ system have been mainly focused on theoretical calculations. There are few methods for preparing $REFe_{1-x}Cr_xO_3$ single phases, as in the case of the ceramic method with repeated grinding and calcinations that the B-site Fe–Cr disorder is concomitant frequently and they separate into Fe oxide and Cr oxide phases.[16]

Hydrothermal synthesis, as well as solvothermal[17] in non-aqueous solvents, is a productive method to prepare versatile materials, such as fine oxide powders,[18] complex oxides of perovskites and pyrochlores,[19] and the crystallization of ceramics.[20] As a soft chemical method with the ability to control various particle sizes and dimensions, it has been widely applied to the synthesis of meta-stable phase crystals.[21] There are many advantages of this method, such as low growth temperature, one-step synthesis procedure, easy handling and controllable particle size distribution,[18,19] so it is desirable in the preparation of crystals. The synthesis of perovskite-type $LaCrO_3$[22–25] and $LaFeO_3$[26,27] *via* a mild hydrothermal method and the conditions of the crystal formation have been reported and examined before. In our previous work, the maximum magnetization (M_{max}) and remnant magnetization (M_r) reached their maximum with a Fe/Cr = 1:1 composition at the B-site.[28] The temperature dependence of the electrical conductivities of $La_{1-x}Sr_xCrO_3$ (x = 0, 0.1, 0.2), prepared by a hydrothermal method, was reported recently.[29] Similar studies have focused on the thermal decomposition method of $LaFeO_3$.[30] The field-induced polar order was recognized in rare earth chromites below the Neel temperature, when the rare earth elements are magnetic.[31] Recent studies have shown that magnetically driven ferroelectricity has been found in

[a] *State Key Laboratory of Inorganic Synthesis and Preparative Chemistry, College of Chemistry, Jilin University, Changchun 130012, P. R. China. E-mail: shfeng@mail.jlu.edu.cn; Fax: +86-431-85168624; Tel: +86-431-85168661*
[b] *Department of Chemistry and Chemical Biology, Rutgers University, Piscataway, New Jersey 08854, USA*

several ferrites and chromites.[32] In this paper, we report a mild and simple hydrothermal method to synthesize single phases of $REFe_{0.5}Cr_{0.5}O_3$ (RE = La, Tb, Ho, Er, Yb, Lu and Y) with the size of several micrometers at a relatively low temperature. Direct current (DC) magnetization *versus* temperature measurements were carried out.

Experimental section

The hydrothermal syntheses of a series of $REFe_{0.5}Cr_{0.5}O_3$ (RE = La, Tb, Ho, Er, Yb, Lu, and Y) materials were undertaken by a single-step process without any precursor preparation. Sample syntheses were carried out in an 18 mL Teflon-lined stainless steel autoclave with a filling capacity of ~80%. Solutions of 0.4 M for each reagent, such as $La(NO_3)_3$, $Tb(NO_3)_3$, $Ho(NO_3)_3$, $Er(NO_3)_3$, $Yb(NO_3)_3$, $Lu(NO_3)_3$, $Y(NO_3)_3$, $Fe(NO_3)_3$ and $CrCl_3$ were prepared in advance before each synthesis. Firstly, 2.5 mL $Fe(NO_3)_3$ and 2.75 mL $CrCl_3$ (10% excess of Cr^{3+} for the oxidation balance in high OH^- concentration) were injected into a beaker with continuous magnetic stirring, to which 1 g KOH was added to form a suspension.

After the suspension cooled to room temperature (heat released by KOH dissolution), 5 mL 0.4 M $RE(NO_3)_3$ solution was dripped in.

Then, another 2–6 g of KOH, as a mineralizer, was added into the beaker to maintain the right concentration for nucleation. A dark crimson suspension formed after adequate vigorous stirring. The suspension was not poured into the Teflon autoclave until it cooled to room temperature. Autoclaves were kept at 240 °C for 5 days and then cooled to room temperature in air. Dark crimson samples sank to the bottom of the solution in the Teflon autoclaves. Deionized water was used to wash the samples to neutralize, and single-phase samples $REFe_{0.5}Cr_{0.5}O_3$ were obtained as fine crystalline powders.

Product composition was determined by inductively coupled plasma spectroscopy (ICP) and confirmed by energy dispersive spectroscopy (EDS). Powder X-ray diffraction (XRD) data were collected on a Rigaku D/Max 2500 V/PC X-ray diffractometer with Cu-Kα radiation (λ = 1.54718 Å) at 50 kV and 200 mA with a scan speed of 1° min^{-1} at room temperature. The step scanning was in the angle range of $20^\circ \leq 2\theta \leq 70^\circ$ with an increment of 0.02°. Pawley refinement was performed with Accelrys MS Modeling software. Scanning electron microscope (SEM) images were obtained with a Helios NanoLab 600i Dual Beam System, FEI Company, America. Hysteresis, zero-field-cooled (ZFC) and field-cooled (FC) magnetization measurements were performed on a superconducting quantum interference device (SQUID) magnetometer (Quantum Design) from 4 to 380 K.

Results and discussion

Compositional analyses by ICP and EDS of the as-made samples demonstrated the chemical formula of $REFe_{0.5}Cr_{0.5}O_3$. All samples were characterized by the room temperature powder XRD and XRD data of the phase-pure samples, which could be well indexed to the orthorhombic perovskite structure with space group *Pbnm*. The XRD patterns and Pawley refinements are shown in Fig. 1(a)–(g). Cell parameters of the as-prepared samples are shown in Fig. 2. The unit cell volume gradually increases with the increase of the ionic radius of the A-site rare-earth elements. The lattice parameters of $LaFe_{0.5}Cr_{0.5}O_3$, $YFe_{0.5}Cr_{0.5}O_3$ are consistent with the previously reported values.[15,28]

The SEM images of the compounds $REFe_{0.5}Cr_{0.5}O_3$ are shown in Fig. 3. All the samples are single phase with uniform sized crystals. The shape of the samples vary from cubic (Fig. 3a) to hexagonal (Fig. 3b) and rhombus plate (Fig. 3c, d and g), then multi-intercalated round plate (Fig. 3e and f), with all of the samples showing no agglomeration compared to the reference reported higher temperature hydrothermal synthesized rare-earth and yttrium orthochromite perovskites.[24] The crystal sizes of the as-made samples are *ca.* 5 μm, 5 μm, 10 μm, 10 μm, 10 μm, 8 μm and 8 μm for $LaFe_{0.5}Cr_{0.5}O_3$ (Fig. 3a), $TbFe_{0.5}Cr_{0.5}O_3$ (Fig. 3b), $HoFe_{0.5}Cr_{0.5}O_3$ (Fig. 3c), $ErFe_{0.5}Cr_{0.5}O_3$ (Fig. 3d), $YFe_{0.5}Cr_{0.5}O_3$ (Fig. 3g), $YbFe_{0.5}Cr_{0.5}O_3$ (Fig. 3e) and Lu $Fe_{0.5}Cr_{0.5}O_3$ (Fig. 3f), respectively.

As a mineralizer, KOH plays a crucial role in controlling the Fe/Cr ratios of the final products of the perovskite structure. The mineralizing effect was also confirmed in the hydrothermal synthesis of other complex transition metal oxides.[33] In this work, we noticed again that the compositions were strongly dependent on the alkalinity of the initial reactant mixture.[28] The effect of the alkalinity may probably be due to the oxidation of the Cr species in solution with different pH values[25] and the difference of precipitation–dissolution equilibrium between $Fe(OH)_3$ and $Cr(OH)_3$. Cr^{3+} can be oxidized to $Cr_2O_7^{2-}$ in the presence of a high concentration of KOH,[25,28] which should avoid any compensation from $Cr(OH)_3$.

The reaction temperature also plays an important role in the formation and crystallinity of the compounds. It was found that the compounds can not be obtained when the reaction temperature is lower than 240 °C.

The temperature dependence of the DC magnetic susceptibility was measured at 1000 Oe for the as-made samples, as shown in Fig. 4. Only an antiferromagnetic transition (Fig. 4a and g) can be confirmed in some samples in the whole temperature range of the measurement. Although ferromagnetism was expected due to the superexchange interaction of the ordered arrangement of $Fe^{3+}(d^5)$–O–$Cr^{3+}(d^3)$–O–$Fe^{3+}(d^5)$ at the B-site, our results showed a complicated interaction for either the B-site of Fe^{3+} and Cr^{3+} or the A-site rare-earth ions (RE^{3+}) and the B-site. Thus, Fe^{3+} and Cr^{3+} ions were distributed randomly at the B-site and the main distribution is $Fe^{3+}(d^5)$–O–$Fe^{3+}(d^5)$, $Cr^{3+}(d^3)$–O–$Cr^{3+}(d^3)$ exchange interactions with only $Fe^{3+}(d^5)$–O–$Cr^{3+}(d^3)$ between the inter-site of the two. This is clearly seen in Fig. 4a and g for $LaFe_{0.5}Cr_{0.5}O_3$ and $YFe_{0.5}Cr_{0.5}O_3$, where the ions on the rare-earth site carry no magnetic moment. The Neel temperature of the other $REFe_{0.5}Cr_{0.5}O_3$ were beyond the measurable range of SQUID. $YFe_{0.5}Cr_{0.5}O_3$ exhibits a magnetic ordering at T_N = 246 K, which is due to the antiferromagnetic coupling of the Fe^{3+} and Cr^{3+} moments.[6,15] The magnetic hysteresis of $YFe_{0.5}Cr_{0.5}O_3$ at 4 and 300 K are shown in Fig. 4h. Compared to the samples prepared by the solid state method,[6,15] the

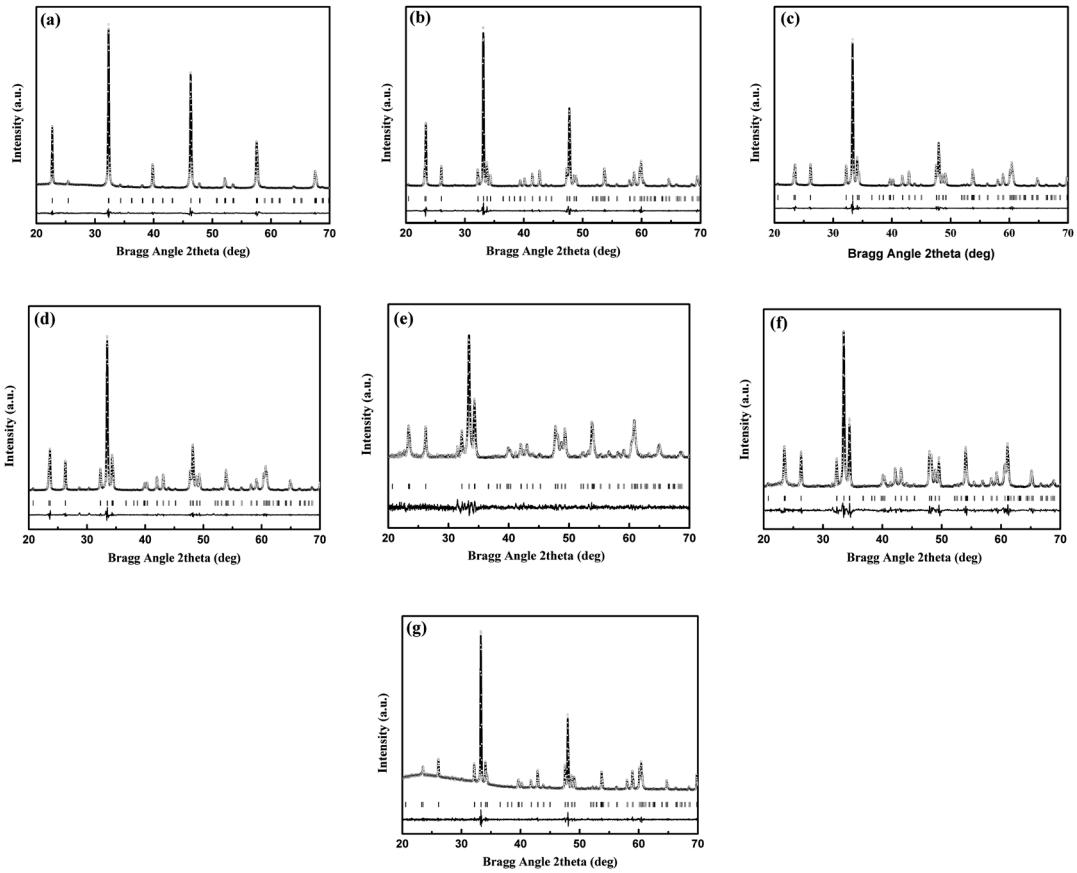

Fig. 1 Pawley refinement of samples as-made (a) $LaFe_{0.5}Cr_{0.5}O_3$, (b) $TbFe_{0.5}Cr_{0.5}O_3$, (c) $HoFe_{0.5}Cr_{0.5}O_3$, (d) $ErFe_{0.5}Cr_{0.5}O_3$, (e) $YbFe_{0.5}Cr_{0.5}O_3$, (f) $LuFe_{0.5}Cr_{0.5}O_3$ and (g) $YFe_{0.5}Cr_{0.5}O_3$ from XRD data. All peaks can be well indexed to orthorhombic *Pbnm*. Observed (○), calculated (—), and difference (bottom) profiles are shown. The Bragg reflection positions are marked with vertical bars.

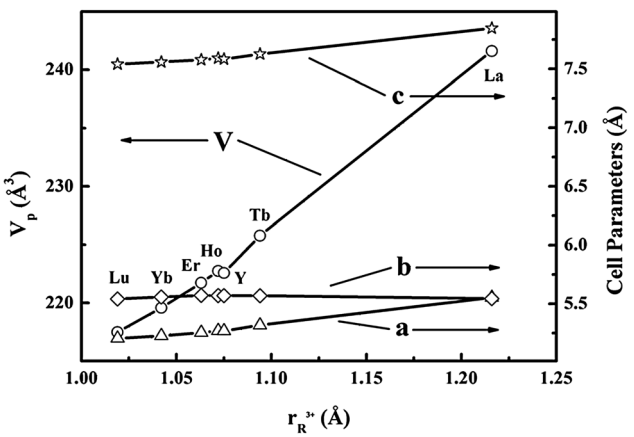

Fig. 2 Variation of cell parameters and primitive unit cell volume (V_p) with effective ionic radius (nine-coordination) of rare-earth half Fe-doped orthochromites synthesized under mild hydrothermal conditions.

magnetization of the maximal and remnant (M_r) susceptibility was improved significantly ($M_r \sim 0.52$ emu g^{-1} at 4 K *vs.* 0.16 emu g^{-1} at 5 K[6]). The improvement of magnetization may be attributed to the enhanced short range magnetic ordering, either from the canting moments in the antiferromagnetic structure[7] or from the superexchange interaction (according to KG rule)[11,12] of the $Fe^{3+}(d^5)$–O–$Cr^{3+}(d^3)$ arrangement in partial order. The room temperature (300 K) *M–H* curve of our sample $YFe_{0.5}Cr_{0.5}O_3$ (inset of Fig. 4h) shows a weak hysteresis, which is not seen in the solid state method prepared samples.[6,7] A similar improvement was also achieved in the $LaFe_{0.5}Cr_{0.5}O_3$ samples.[28] Accordingly, partial Fe–O–Cr FM ordering can be achieved in the samples from the hydrothermal systems. For all other materials prepared, the rare-earth ions (RE^{3+}) also carry a magnetic moment,[34] which may couple with the B-site ion spin structure.

Paramagnetism at a temperature above the critical point can be seen from the inset of Fig. 4a–e and g, while below that, a complicated interaction in each of samples occurred. A cusp occurs in $TbFe_{0.5}Cr_{0.5}O_3$ (Fig. 4b) and $YbFe_{0.5}Cr_{0.5}O_3$ (Fig. 4e) at 52 K and 44 K, respectively, which may be related to the complex interactions[35] between the 4f electrons of Tb^{3+}/Yb^{3+} and 3d electrons of Fe^{3+} and Cr^{3+}. The transition temperature of the other samples was not observed in the temperature range. For $HoFe_{0.5}Cr_{0.5}O_3$ (Fig. 4c) and $ErFe_{0.5}Cr_{0.5}O_3$ (Fig. 4d), ZFC and FC curves merged at ~153.6 K and ~165.6 K, respectively. However, in $LuFe_{0.5}Cr_{0.5}O_3$ (Fig. 4f), rather complex ZFC and FC curves were shown, which may originate from the small radius[34] of Lu^{3+} and reduced bond angle of B–O–B, and thus enforce the interactions of both. Further evidence is needed to investigate this question.

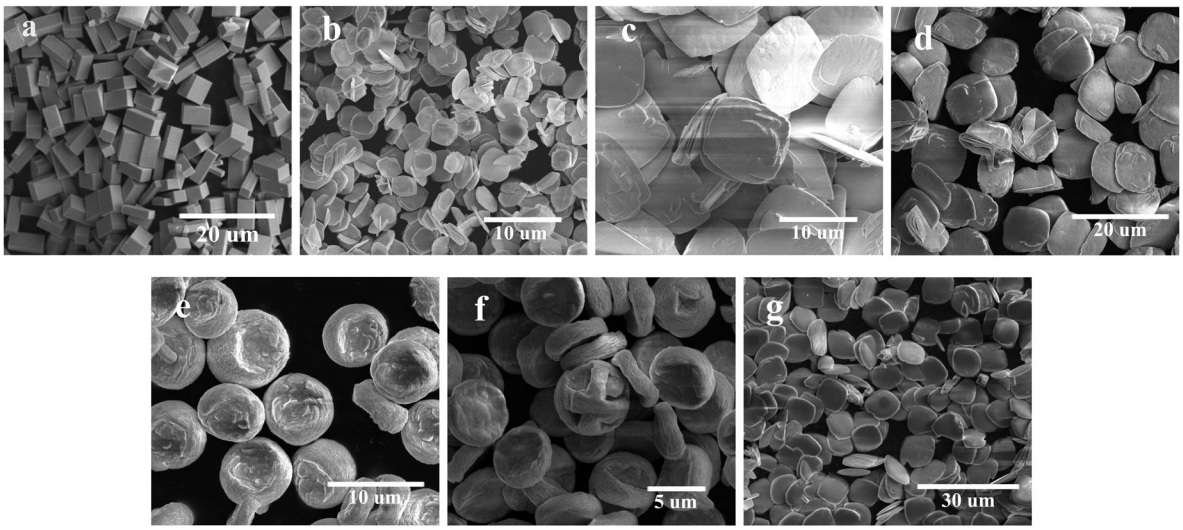

Fig. 3 SEM images of the samples: (a) $LaFe_{0.5}Cr_{0.5}O_3$, (b) $TbFe_{0.5}Cr_{0.5}O_3$, (c) $HoFe_{0.5}Cr_{0.5}O_3$, (d) $ErFe_{0.5}Cr_{0.5}O_3$, (e) $YbFe_{0.5}Cr_{0.5}O_3$, (f) $LuFe_{0.5}Cr_{0.5}O_3$, (g) $YFe_{0.5}Cr_{0.5}O_3$.

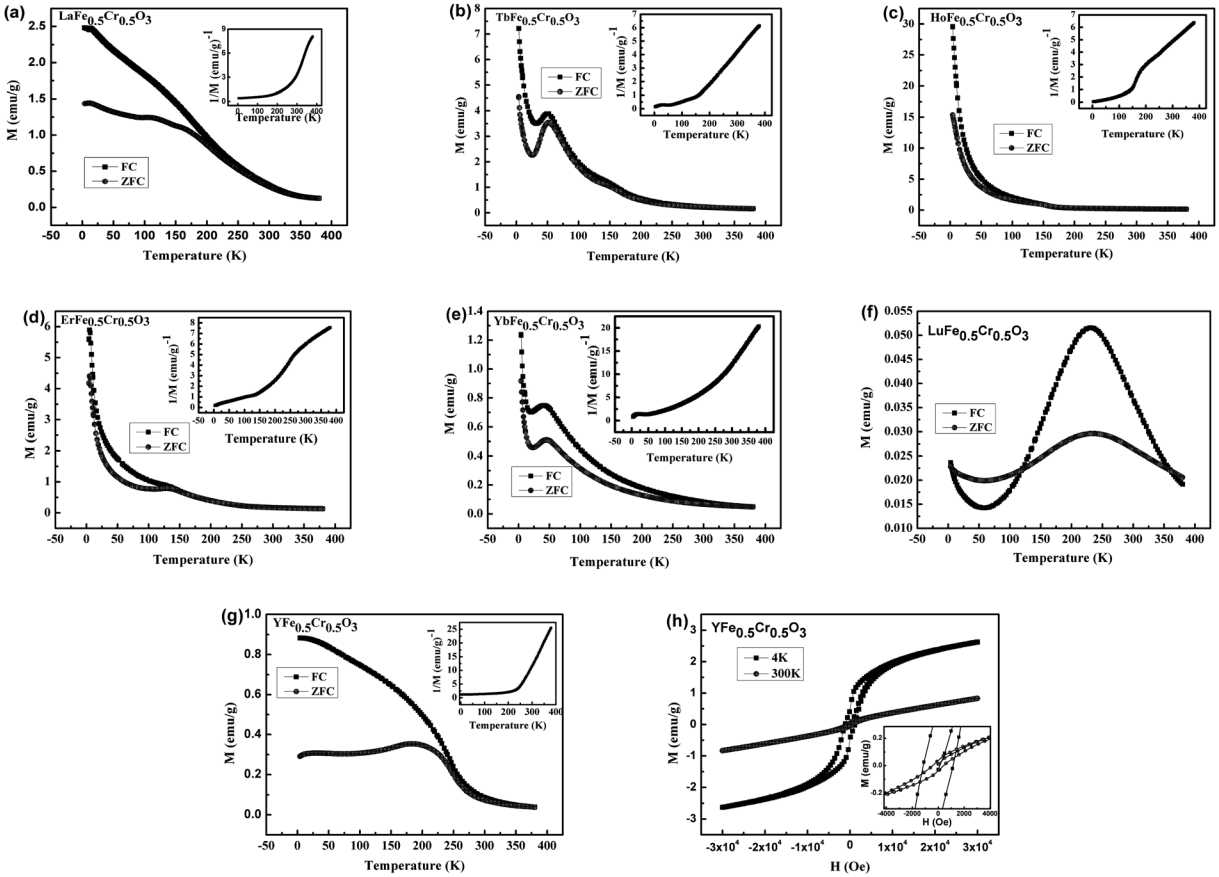

Fig. 4 Temperature dependence of magnetization (ZFC and FC) of the $ReFe_{0.5}Cr_{0.5}O_3$ samples at 0.1 T: (a) $LaFe_{0.5}Cr_{0.5}O_3$, (b) $TbFe_{0.5}Cr_{0.5}O_3$, (c) $HoFe_{0.5}Cr_{0.5}O_3$, (d) $ErFe_{0.5}Cr_{0.5}O_3$, (e) $YbFe_{0.5}Cr_{0.5}O_3$, (f) $LuFe_{0.5}Cr_{0.5}O_3$ and (g) $YFe_{0.5}Cr_{0.5}O_3$ (the inset of (a)–(e) and (g) shows the temperature dependence of the 1/*M* curves), (h) hysteresis of $YFe_{0.5}Cr_{0.5}O_3$.

Conclusions

In summary, Fe half-doped rare-earth chromite perovskite structure samples were prepared *via* a one-pot mild hydrothermal route. The KOH concentration and temperature played an essential role in the crystal formation. The lattice parameters were increased with the radius of the rare-earth elements. The field-cooled (FC) and zero-field-cooled (ZFC) direct magnetizations indicated

complex interactions in all our samples. A higher ordered arrangement of Fe and Cr at the B-site was achieved in $YFe_{0.5}Cr_{0.5}O_3$ in this method.

Acknowledgements

This work was supported by the National Natural Science Foundation of China (Grants 90922034, 21131002 and 21201075) and the Specialized Research Fund for the Doctoral Program of Higher Education (SRFDP Grant 20110061130005). Gratitude to Lei Ge, PhD candidate of Jilin University, for the magnetization measurement.

References

1 K. Ueda, H. Tabata and T. Kawai, *Science*, 1998, **280**, 1064–1066.
2 K. Miura and K. Terakura, *Phys. Rev. B: Condens. Matter Mater. Phys.*, 2001, **63**, 104402.
3 T. Ramos, M. D. Carvalho, L. P. Ferreira, M. M. Cruz and M. Godinho, *Chem. Mater.*, 2006, **18**, 3860–3865.
4 M. E. Villafuerte-Castrejón, M. García-Guaderrama, L. Fuentes, J. Prado-Gonjal, A. M. González, M. Á. de la Rubia, M. García-Hernández and E. Morán, *Inorg. Chem.*, 2011, **50**, 8340–8347.
5 J. R. Sahu, C. R. Serrao, N. Ray, U. V. Waghmare and C. N. R. Rao, *J. Mater. Chem.*, 2007, **17**, 42–44.
6 B. Rajeswaran, P. Mandal, R. Saha, E. Suard, A. Sundaresan and C. N. R. Rao, *Chem. Mater.*, 2012, **24**, 3591–3595.
7 V. G. Nair, A. Das, V. Subramanian and P. N. Santhosh, *J. Appl. Phys.*, 2013, **113**, 213907.
8 C. R. Serrao, A. K. Kundu, S. B. Krupanidhi, U. V. Waghmare and C. N. R. Rao, *Phys. Rev. B: Condens. Matter Mater. Phys.*, 2005, **72**, 220101.
9 V. M. Judin, A. B. Sherman and I. E. Myl'nikova, *Phys. Lett.*, 1966, **22**, 554–555.
10 G. Gorodetsky, S. Shtrikman and D. Treves, *Solid State Commun.*, 1966, **4**, 147–151.
11 J. Kanamori, *J. Phys. Chem. Solids*, 1959, **10**, 87–98.
12 J. B. Goodenough, *Phys. Rev.*, 1955, **100**, 564–573.
13 M. V. Kuznetsov, Q. A. Pankhurst, I. P. Parkin and Y. G. Morozov, *J. Mater. Chem.*, 2001, **11**, 854–858.
14 H. Taguchi, *J. Solid State Chem.*, 1997, **131**, 108–114.
15 A. Dahmani, M. Taibi, M. Nogues, J. Aride, E. Loudghiri and A. Belayachi, *Mater. Chem. Phys.*, 2003, **77**, 912–917.
16 A. Wold and W. Croft, *J. Phys. Chem.*, 1959, **63**, 447–448.
17 G. Demazeau, *J. Mater. Chem.*, 1999, **9**, 15–18.
18 S. Sōmiya and B. Roy, *Bull. Mater. Sci.*, 2000, **23**, 453–460.
19 D. R. Modeshia and R. I. Walton, *Chem. Soc. Rev.*, 2010, **39**, 4303–4325.
20 R. E. Riman, W. L. Suchanek and M. M. Lencka, *Ann. Chim. Sci. Mater.*, 2002, **27**(6), 15–36.
21 S. H. Feng and R. R. Xu, *Acc. Chem. Res.*, 2001, **34**, 239–247.
22 M. Yoshimura, S. T. Song and S. Sōmiya, *J. Ceram. Soc. Jpn.*, 1982, **2**, 91–95.
23 S. T. Song, H. Y. Pan, Z. Wang and B. Yang, *Ceram. Int.*, 1984, **10**, 143–146.
24 K. Sardar, M. R. Lees, R. J. Kashtiban, J. Sloan and R. I. Walton, *Chem. Mater.*, 2011, **23**, 48–56.
25 W. J. Zheng, W. Q. Pang, G. Y. Meng and D. K. Peng, *J. Mater. Chem.*, 1999, **9**, 2833–2836.
26 M. Yoshimura, K. Yamasawa and S. Sōmiya, *Proceedings of the International Meeting on Chemical Sensors*, 1983, 198–202.
27 W. Zheng, R. Liu, D. Peng and G. Meng, *Mater. Lett.*, 2000, **43**, 19–22.
28 W. W. Hu, Y. Chen, H. M. Yuan, G. H. Zhang, G. H. Li, G. S. Pang and S. H. Feng, *J. Solid State Chem.*, 2010, **183**, 1582–1587.
29 S. Wang, K. K. Huang, B. N. Zheng, J. Q. Zhang and S. H. Feng, *Mater. Lett.*, 2013, **101**, 86–89.
30 S.-H. Chung, K.-C. Chiu and J.-H. Jean, *Jpn. J. Appl. Phys.*, 2008, **47**, 8498–8501.
31 B. Rajeswaran, D. I. Khomskii, A. K. Zvezdin, C. N. R. Rao and A. Sundaresan, *Phys. Rev. B: Condens. Matter Mater. Phys.*, 2012, **86**, 214409.
32 C. N. R. Rao, A. Sundaresan and R. Saha, *J. Phys. Chem. Lett.*, 2012, **3**, 2237–2246.
33 Y. Chen, H. M. Yuan, G. H. Li, G. Tian and S. H. Feng, *J. Cryst. Growth*, 2007, **305**, 242–248.
34 J. Prado-Gonjal, R. Schmidt, J.-J. Romero, D. Ávila, U. Amador and E. Morán, *Inorg. Chem.*, 2013, **52**, 313–320.
35 Y. Su, J. Zhang, Z. Feng, L. Li, B. Li, Y. Zhou, Z. Chen and S. Cao, *J. Appl. Phys.*, 2010, **108**, 013905.

